

Diffusion and multistage kinetics of macromolecular adsorptionTom Chou^{1,2} and Maria R. D'Orsogna²¹ Dept. of Biomathematics, UCLA, Los Angeles, CA 90095-1766² Dept. of Mathematics, UCLA, Los Angeles, CA 90095-1555

(Dated: February 8, 2020)

We derive the equations that describe adsorption of diffusing particles onto a surface followed by additional surface kinetic steps before being transported across the interface. Multistage surface kinetics occurs during membrane protein insertion, cell signaling, and the infection of cells by virus particles. For example, after nonspecific binding, additional kinetic steps, such as binding of receptors and coreceptors, must occur before virus particle fusion can occur. We couple the diffusion of particles in the bulk phase with the surface kinetics and derive an effective, integro-differential boundary condition that contains a memory kernel describing the delay induced by the surface reactions. This boundary condition takes the form of a singular perturbation problem in the limit where particle-surface interactions are short-ranged. Moreover, depending on the surface kinetics, the delay kernel induces a nonmonotonic, transient replenishment of the bulk particle concentration near the interface. Our approach generalizes that of Ward and Tordai [1] and Diamant and Andelman [2] to include surface kinetics, giving rise to qualitatively new behaviors.

PACS numbers: 68.43.+h, 87.68.+z, 68.47.Pe, 68.03.+g

I. INTRODUCTION

Adsorption of particles onto interfaces, and transport through them, arise in numerous biological and engineering processes, playing a key role in surfactant adsorption [3, 4], membrane biology and cell signaling [5–10], and even marine layer oceanography [11]. Particle adsorption may fundamentally alter the physical and chemical properties of the interface, and it is crucial to understand both equilibrium and dynamical properties of the adsorbed layers [1, 3, 4, 6]. In the seminal work of Ward and Tordai [1], a bulk phase acting as a reservoir of particles is bounded by an initially empty surface onto which the particle adsorb. Particles are assumed to lower their free energy with respect to the bulk by irreversibly and instantaneously adsorbing onto the interface. Under these conditions, the total concentration of adsorbed particles may be calculated in terms of measurable interfacial properties, such as the dynamic surface tension. Several applications, extensions and alternate approaches to this work have been proposed. In particular, adsorption dynamics in the Ward-Tordai setting can be rederived through a free energy approach [2], allowing for the inclusion of ionic surfactant effects and electrostatic interactions.

In many biochemical systems, the complete adsorption of a particle arriving from the bulk often requires a series of transformations at the surface before the particle can be successfully annihilated, or fused into the surface. These intermediate steps gives rise to a lag-time in the complete adsorption process. For example, the incorporation of emulsi-

fyng proteins onto an air-water interface is delayed possibly by the unfolding of the polypeptide at the interface [7]. Delays have also been observed in the adsorption of the hemagglutinin glycoprotein (HA) of the influenza virus as it enters target host cellular membranes [12]. The mechanisms underlying this delay are not known in detail but are believed to involve conformational changes of HA molecules into fusion enabling complexes, or the presence of receptors and coreceptors at the binding site [12–14]. Similarly, the incorporation of an HIV particle into a cell is possible only after the virus glycoprotein gp120 recognizes and binds to the surface receptor CD4, and subsequently to a series of coreceptors, CCR5 or CXCR4. As in the case of HA and influenza, the exact molecular intermediates required for HIV particle fusion are yet unknown and might depend on gp120 conformations and receptor/coreceptor binding cooperativity [15, 16]. The complex nature of surface biochemistry makes quantitative kinetic measurements challenging. Recently, the binding kinetics of the CD4 receptor to the gp120 ligand have been measured under different experimental conditions yielding widely different dissociation rates [17, 18]. In this work, we will provide a quantitative framework that can be used to better understand measurements of surface kinetics that involve multistage surface chemistry.

We will explicitly consider the intermediate, reversible steps for surface binding in the Ward-Tordai formalism, introducing the effective boundary conditions to complement the bulk diffusion process. As we shall see, the need for auxiliary surface species to correctly bind to the putative fusion site, will

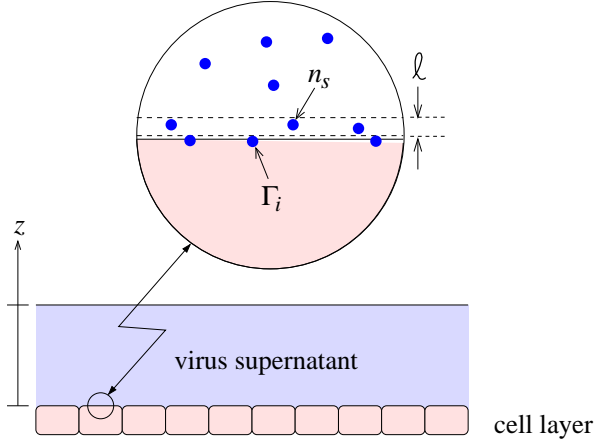


FIG. 1: A schematic of a typical adsorption experiment on a confluent monolayer of target cells. Particles such as viruses are spread over the cell layer in a thin film. After initial nonspecific adsorption, receptors and coreceptors bind via a complex stoichiometry, subsequently forming fusion-competent species (not shown). The subsurface layer of thickness ℓ , the subsurface concentration $n_s(t)$, and initial nonspecifically adsorbed species Γ_1 are discussed below.

effectively introduce a lag time between the initial surface binding event and the final fusion process. Our analysis can be readily applied to the titration of replication-incompetent virus via a colony formation assay as shown in Fig. 1 [19].

II. DIFFUSION AND EFFECTIVE BOUNDARY CONDITIONS

In the continuum limit, the density of particles $n(\mathbf{r}, t)$ in the bulk phase, obeys the convection-diffusion equation

$$\frac{\partial n(\mathbf{r}, t)}{\partial t} = \nabla \cdot [D(\mathbf{r}) \nabla n(\mathbf{r}, t)] + \nabla \cdot \left[\frac{D(\mathbf{r})}{k_B T} n(\mathbf{r}, t) \nabla U(\mathbf{r}) \right]. \quad (1)$$

where $D(\mathbf{r})$ and $U(\mathbf{r})$ are the local diffusion coefficient and potential of mean force, respectively, and $k_B T$ is the thermal energy. The variation of $D(\mathbf{r})$ and $U(\mathbf{r})$ may arise from interactions with the interface as schematically depicted in Figure 3. Boundary conditions are typically applied at the mathematical surface onto which the particles adsorb or reflect. By considering the flux through this mathematical interface, one generally arrives at a mixed boundary condition of the form:

$$D(\mathbf{r}) \mathbf{n} \cdot \nabla n(\mathbf{r}, t) = \gamma n(\mathbf{r}, t), \quad \mathbf{r} \in \mathbf{S}. \quad (2)$$

where $\gamma \propto f/(1-f)$ and f is the probability that a particle is adsorbed into the mathematical interface upon collision. The latter is also known as the sticking probability [20, 21] and has been applied to related models of gas adsorption on solid substrates [21]. In the limit $f \rightarrow 1$, Eq. 2 is equivalent to $n(\mathbf{r} \in \mathbf{S}) = 0$, a Dirichlet boundary condition. A Neumann boundary condition, $\mathbf{n} \cdot \nabla n = 0$, arises when $f = 0$. Equations 1 and 2 are commonly used to model simple diffusion-adsorption processes at surfaces.

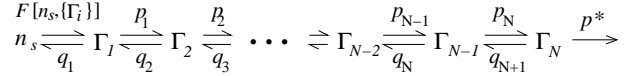


FIG. 2: Surface reaction scheme among the intermediate states Γ_i . The source for Γ_1 , the initial adsorbed species is the bulk surface concentration at the interface n_s . In the context of virus recognition and infection, the intermediate steps label various numbers of receptors or coreceptors associated with the surface bound virus particle. For example, Γ_i may be the surface concentration of HIV particles with i CD4 receptors attached. Subsequent attachment of additional coreceptors such as CCR5 may also be included in the chain of intermediates Γ_i .

In many applications, one is also interested in the surface concentration $\Gamma(t)$ of particles adsorbed on the interface, and how this surface concentration can alter the mechanical properties of the interface. A well studied system has been the dynamic surface tension controlled by the surface concentration of surfactants [1–4] or proteins [6, 7] at fluid-fluid interfaces. Solid state examples include adsorption of thiols on gold surfaces [20]. The surface species may undergo further chemical modification, particularly in biochemical settings. We include these additional kinetic steps at the surface by assuming N possible surface species Γ_i , $1 \leq i \leq N$, for example representing the ligand with various numbers of bound receptors/coreceptors. Immediately after adsorption from the bulk, the surface ligand concentration, denoted Γ_1 , can evolve into the other species Γ_i . This will be modeled with a linear rate equation $\partial_t \mathbf{\Gamma} = \mathbf{M} \mathbf{\Gamma} + \mathbf{F}(t)$, where $\mathbf{\Gamma} \equiv (\Gamma_1, \Gamma_2, \dots, \Gamma_N)$, \mathbf{M} is the transition matrix among the N surface states, and $\mathbf{F} \equiv (F, 0, \dots, 0)$ is the source of Γ_1 coming from the bulk. Figure 2 depicts an example of a surface reaction scheme that can be describe by the above linear rate equation and which we will analyze in detail later.

In order to couple the surface densities Γ_i (number per area) to the bulk densities $n(\mathbf{r}, t)$ (number per volume) near the interface, an additional kinetic model is required near the interface. We thus introduce a thin layer of thickness ℓ near the surface, in

which the particle density is denoted by $n_s(t)$ and is still expressed in units of number per volume. Others also introduce the sublayer as a mathematical step coupling the bulk density to surface density [2]. Here, we physically motivate this subsurface layer and the associated kinetics between the bulk and surface densities before presenting the complete mathematical problem.

An intrinsic length scale ℓ that might define this sublayer thickness arises when the continuum approximation Eq. 1 breaks down. This occurs at distances of the order of a few mean free paths of the diffusing particle as shown in Fig. 3. If we assign the layer thickness $\ell = \ell_{mfp}$, we must solve Eq. 1 with a nonuniform $U(\mathbf{r})$ and possibly $D(\mathbf{r})$ to within a distance ℓ of the interface. The value of the bulk density at the boundary $\mathbf{S} + \ell\mathbf{n}$ is defined as the sublayer density: $n(\mathbf{r} = \mathbf{S} + \ell\mathbf{n}, t) = n_s(t)$. The equation for the rate of change of the number per area of molecules in the thin layer, $d(\ell n_s(t))/dt$ can be obtained by balancing it with the diffusive flux into the layer $D(\mathbf{r}) \mathbf{n} \cdot \nabla n(\mathbf{S} + \ell\mathbf{n}, t)$, the adsorption into the surface concentration Γ_1 , and the spontaneous desorption from the initially adsorbed species Γ_1 that occurs at rate q_1 .

The complete set of equations coupling the variables $n(\mathbf{r}, t)$, $n_s(t)$, and Γ_i is thus

$$\frac{\partial n(\mathbf{r}, t)}{\partial t} = \nabla \cdot [D(\mathbf{r}) \nabla n(\mathbf{r}, t)] + \nabla \cdot \left[\frac{D(\mathbf{r})}{k_B T} n(\mathbf{r}, t) \nabla U(\mathbf{r}) \right], \quad (3)$$

$$\begin{aligned} \ell \frac{dn_s(t)}{dt} &= -F + D(\mathbf{r}) \mathbf{n} \cdot \nabla n(\mathbf{r}, t) \Big|_{\mathbf{r}=\mathbf{S}+\ell\mathbf{n}} + q_1 \Gamma_1(t), \\ n(\mathbf{S} + \ell\mathbf{n}, t) &= n_s(t) \end{aligned} \quad (4)$$

$$\frac{d\Gamma(t)}{dt} = \mathbf{M}\Gamma + \mathbf{F}(t), \quad \mathbf{F} = (F, 0, 0, \dots, 0). \quad (5)$$

Here, $F = F[n_s, \{\Gamma_i\}]$ describes the rate of adsorption of the n_s species into the incipiently adsorbed species Γ_1 . This function may depend on interactions, including crowding, with all other surface species Γ_i and may be modeled using free energies and chemical potential differences between the bulk and surface [2].

To simplify the analysis further, one can take the sublayer thickness to be $\ell = \ell_{int}$, the typical maximum range of the particle-surface interaction as shown in Fig. 3. If the sublayer extends beyond the interface potential of mean force, $D(\mathbf{r})$ is constant, $U(\mathbf{r}) = 0$, and Eq. 1 simplifies to

$$\frac{\partial n(\mathbf{r}, t)}{\partial t} = D \nabla^2 n(\mathbf{r}, t). \quad (6)$$

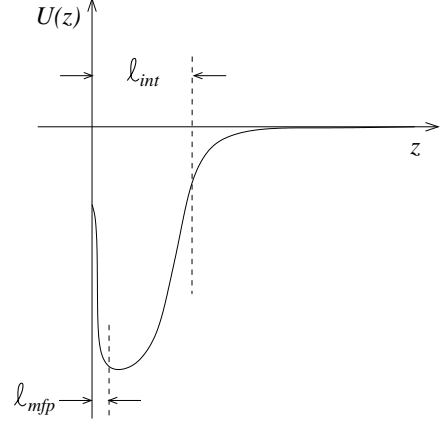


FIG. 3: Interaction potential between diffusing species and the interface. The subsurface layer is defined by either the range of the interaction potential ℓ_{int} , or the mean free path ℓ_{mfp} , depending upon which is larger.

All effects of the potential of mean force $U(\mathbf{r})$ and spatially varying $D(\mathbf{r})$ are now buried within $F[n_s, \{\Gamma_i\}]$. This is consistent with all previous treatments [1, 2, 4] in which transport in the bulk phase was described by simple diffusion with uniform D and U . Provided $F[n_s(t)]$ is independent of Γ_i , equations 1-5 can be explicitly solved in simple geometries. For low surface densities Γ_i such that additional adsorption is not hindered by steric exclusion, one can assume a linear form $F[n_s] = \gamma n_s(t)$, independent of Γ_i . For the choice of sublayer thickness $\ell = \ell_{mfp}$, the adsorption rate γ can be approximated by the sticking probability times the thermal velocity of the particle near the interface. If one chooses $\ell = \ell_{int}$, the adsorption kinetics can still be modeled as $F[n_s] \approx \gamma n_s(t)$. However, γ is now interpreted as an effective adsorption rate allowing Eq. 1 to be replaced by Eq. 6, and simplifying the bulk concentration equation.

Previous studies on adsorption and dynamic surface tension measurements [1, 4] eliminate the bulk density at the interface in Eq. 4 to yield two coupled integro-differential equations for n_s and Γ_1 which must be numerically solved self-consistently. Instead, we solve the linear equations 5 independently from the bulk densities, but with a source term $F[n_s]$ that connects the surface concentrations Γ_i with the bulk concentration $n(\mathbf{r}, t)$. If $F[n_s]$ is independent of Γ_i , the solution to Eqs. 5 is

$$\Gamma(t) = \sum_{m=1}^N \mathbf{v}^m \mathbf{v}^m \cdot \left[\Gamma(0) e^{\lambda_m t} + \int_0^t \mathbf{F}(t') e^{\lambda_m(t-t')} dt' \right], \quad (7)$$

where λ_m and \mathbf{v}^m are the eigenvalues and eigen-

vectors of \mathbf{M} . For the case of zero initial surface concentration, $\Gamma(t=0) = 0$, and $\Gamma(t)$ is proportional to $F[n_s(t)]$. Upon substitution of the solution $\Gamma_1(t)$ into Eq. 4, we find a concise description of the diffusion-adsorption process:

$$\frac{\partial n(\mathbf{r}, t)}{\partial t} = D\nabla^2 n(\mathbf{r}, t), \quad n(\mathbf{r} = \mathbf{S} + \ell\mathbf{n}, t) = n_s(t), \quad (8)$$

$$\ell \frac{dn_s(t)}{dt} = D\mathbf{n} \cdot \nabla n(\mathbf{r}, t) \Big|_{\mathbf{r}=\mathbf{S}+\ell\mathbf{n}} + \int_0^t K(t-t')F[n_s(t')]dt', \quad (9)$$

$$K(t) = -\delta(t) + q_1 \sum_{m=1}^N (v_1^m)^2 e^{\lambda_m t}, \quad (10)$$

where $K(t)$ is the kernel constructed from the eigenvalues and eigenvectors of \mathbf{M} . It is composed of an instantaneous response – the immediate depletion of n_s due to adsorption into the Γ_1 surface species – and delay terms arising from the surface kinetics of Eqn. 5. The complete set of equations 8-10 is one of our main findings. This result explicitly shows how multistage adsorption is modeled by a bulk diffusion equation with an nonlinear integro-differential boundary condition that incorporates the delay arising from the multistep kinetics.

The surface densities $\Gamma_i(t)$ can be found by substituting the solution $n_s(t)$ into Eq. 7. Note that Eq. 9 is a singular perturbation in the boundary condition and that for times $t \gg \ell/\gamma$, the ‘‘outer solution’’ approximation $\ell(dn_s/dt) \approx 0$ yields the standard mixed boundary condition Eq. 2 with an additional memory kernel. Furthermore, in the linear approximation, $F[n_s(t)] = \gamma n_s(t)$, the convolution of the delay term in the effective boundary condition 9 is amenable to analysis by Laplace transforms.

Let us assume a simple one-dimensional problem where all quantities vary spatially only in the direction normal to a flat surface at $z = 0$. To simplify our analysis, we nondimensionalize all quantities by using ℓ as the unit of length, and q_1^{-1} as the unit of time. Henceforth, in all equations, we make

the replacements $z \rightarrow z/\ell$, $t \rightarrow q_1 t$, $n \rightarrow \ell^3 n$, $n_s \rightarrow \ell^3 n_s$, $\Gamma_i \rightarrow \ell^2 \Gamma_i$, $D \rightarrow \ell^{-2} D/q_1$, and $\gamma \rightarrow \gamma/(\ell q_1)$.

Upon taking Laplace transforms in time of the dimensionless forms of Eqs. 8, 9, and 10, we obtain

$$sn(z, s) - n_0 = D\partial_z^2 n(z, s), \quad (11)$$

$$sn_s(s) - n_0 = D\partial_z n(z, s) \Big|_{z=1} + \gamma K(s)n_s(s), \quad (12)$$

$$K(s) = -1 + \sum_{m=1}^N \frac{(v_1^m)^2}{s - \lambda_m}, \quad (13)$$

where n_0 is the initial, dimensionless constant bulk and sublayer concentration. The general solution to Eq. 11 is $n(z, s) = n_0/s + A(s) \exp(-z\sqrt{s/D})$, where $A(s)$ is a coefficient determined by substitution into Eq. 12. The solution becomes

$$\frac{n(z, s)}{n_0} = \frac{1}{s} + \frac{\gamma K(s) \exp\left(-z\sqrt{s/D}\right)}{s(s + \sqrt{sD} - \gamma K(s))}, \quad (14)$$

from which the bulk density, and all other quantities, can be found by inverse Laplace transforming $n(z, s)$. If there are no spontaneous source of the surface intermediates, all $\lambda_m < 0$, and one can show that $n(s, z)$ has only a simple pole at $s = 0$ and a branch cut on $s = (-\infty, 0]$. Performing the integral along the branch cut, we find the exact results

$$\frac{n(z, t)}{n_0} = \int_0^\infty L(z, u) e^{-ut} du, \quad (15)$$

and

$$\frac{\Gamma(t)}{\gamma n_0} = \sum_{m=1}^N v^m v_1^m \int_0^\infty \frac{e^{\lambda_m t} - e^{-ut}}{u + \lambda_m} L(1, u) du, \quad (16)$$

where

$$L(z, u) \equiv \frac{\gamma (u + \gamma K(-u)) \sin \sqrt{\frac{u}{D}}(z-1) - \sqrt{uD} \cos \sqrt{\frac{u}{D}}(z-1)}{\pi u(u + \gamma K(-u))^2 + Du^2} K(-u). \quad (17)$$

The short time behavior $n_s(t)/n_0 \sim (1 - \gamma t)$ is

independent of the surface reactions since the initial

steps are adsorption onto the interface with rate γ . For large distances $(z-1)/\sqrt{Dt} \gg 1$ and $\gamma K(s=0) \equiv \gamma K_0 \gg \sqrt{D/t}$, asymptotic evaluation of the Bromwich integral over $n(z, s)$ yields

$$\frac{n(z, t)}{n_0} \sim 1 - \left(1 - \frac{\sqrt{\pi D}}{\gamma K_0 \sqrt{t}}\right) \exp\left[-\frac{(z-1)^2}{4Dt}\right], \quad \frac{z}{\sqrt{Dt}} \gg 1. \quad (18)$$

The leading term on the right-hand-side above is also independent of the surface kinetics. Away from the interface, only information about the initial depletion of n_s has reached large distances.

In the $t \rightarrow \infty$ limit, the dominant contribution to $n(z, t)$ comes from small values of u in Eq. 15. Approximating $L(1, u)$ with its $u \rightarrow 0$ limit, we find the asymptotic long time limit

$$\frac{n_s(t)}{n_0} \sim \frac{1}{\sqrt{t}} \left[\frac{\sqrt{D}}{\gamma \sqrt{\pi} \left(1 + \sum_{m=1}^N \frac{(v_T^m)^2}{\lambda_m}\right)} \right]. \quad (19)$$

This expression is valid only if the surface dynamics include a net sink of material. As long as there is some annihilation, $K_0 = -1 - \sum_{m=1}^N (v_T^m)^2 / \lambda_m < 0$ and Eq. 19 holds. A similar consideration of Eq. 16 yields for the surface concentrations

$$\Gamma(t \rightarrow \infty) \sim \frac{\mathbf{v}_m}{\pi} \frac{n_0 \sqrt{D} e^{\lambda_* t}}{\sqrt{|\lambda_*|} \left(1 + \sum_{m=1}^N \frac{(v_T^m)^2}{\lambda_m}\right)}, \quad (20)$$

where $\lambda_* < 0$ is the largest eigenvalue of the transition matrix \mathbf{M} . These general results rely only on the linearity of $F[n_s]$. They are valid for any surface reaction scheme through the eigenvalues and eigenvectors of the transition matrix M and the resulting function $K(s)$.

We now specify a surface reaction scheme and its associated eigenvalues and eigenvectors and delay kernel. For applications such as multiple receptor binding of the adsorbed species, we consider a reversible sequential Markov process among N chemical intermediates Γ_i , $i = 1, \dots, N$. As shown in Fig. 2, formation of state Γ_{i+1} from state Γ_i occurs at rate p_i , while the reverse step occurs at rate q_{i+1} . The final state Γ_N is irreversibly annihilated, by transport across the membrane, or by irreversible reaction, with rate p^* . We can then explicitly write Eq. 5 with a tridiagonal transition matrix \mathbf{M} as follows

$$\begin{aligned} \frac{d\Gamma_1}{dt} &= F[n_s, \{\Gamma_i\}] - (p_1 + q_1)\Gamma_1 + q_2\Gamma_2, \\ \frac{d\Gamma_i}{dt} &= p_{i-1}\Gamma_{i-1} - (q_i + p_i)\Gamma_i + q_{i+1}\Gamma_{i+1}, \quad 2 \leq i \leq N-1 \\ \frac{d\Gamma_N}{dt} &= -(p^* + q_N)\Gamma_N + p_{N-1}\Gamma_{N-1}. \end{aligned} \quad (21)$$

In the simplest case where there is only one surface intermediate before transport across the interface, $N = 1$ and $K(s) = -(s + p^*) / (s + p^* + 1)$. The sublayer concentration $n_s(t)$ computed from Eq. 15, and the surface concentration computed from Eq. 16 are shown in Fig. 4(a) for various values of γ . For a virus particle of diameter 100nm, its physical diffusion constant is $\sim 10^{-8} \text{cm}^2/\text{s}$. Using the typical screened electrostatic interaction potential, $\ell \approx 10^{-7} \text{cm}$, we estimate the dimensionless diffusion coefficient $D \sim 10^6 \text{s}^{-1}/q_1$. On the other hand, for small ligand molecules $D \sim 10^8 \text{s}^{-1}/q_1$. Values of γ can be estimated using the thermal velocity v_T as $\gamma \approx f v_T / (\ell q_1)$ where f is the sticking probability weighted by the receptor area fraction. For virus particles $\gamma \sim 10^8 \text{s}^{-1} f / q_1$, while for molecular ligands $\gamma \sim 10^{10} \text{s}^{-1} f / q_1$. The dissociation rate q_1 is highly variable and typically falls in the range $q_1 \sim 10^{-4} - 10^4 \text{s}^{-1}$. For the gp120-CD4 interaction, the dissociation has been estimated in model systems to be $q_1 \sim 10^{-3} \text{s}^{-1}$ [17], while mutants can have $q_1 \sim 10^3 \text{s}^{-1}$ [18]. Dissociation rates can be even smaller in tighter binding ligand receptor pairs such as EGF-receptor $q_1 \sim 10^{-4} \text{s}^{-1}$ [22]. For others such as P-selectin and its receptor, $q_1 \sim 0.1 - 1 \text{s}^{-1}$ [23, 24]. The sticking probability is proportional to the binding probability of upon ligand-receptor contact, multiplied by the receptor area fraction at the interface. The factor f depends on the receptor density, but is typically $f \sim 10^{-4} - 10^{-2}$.

Figure 4(a) shows the surface concentration n_s for $p^* = 1$, $N = 1$, and various γ . The sublayer density starts at its initial value n_0 and decreases with rate proportional to γ , eventually monotonically reaching $n_s(t \rightarrow \infty) \rightarrow 0$. If the annihilation rate p^* is decreased, n_s may no longer be monotonic. This is due to the slow consumption of material at the interface, allowing some of the material to desorb after being delayed at the interface. For $p^* = 0.1$, n_s first decreases but recovers slightly at longer times, before ultimately decaying to zero (Fig. 4(b)). This bump arises from the build-up of Γ_1 as shown in Fig. 4(c) which gets released back into the sub-surface layer. For smaller p^* , Γ_1 reaches larger values. As long as $p^* > 0$, both n_s and Γ_1 vanish as sufficiently long times. Note that the curves for n_s exhibit a boundary layer determined by $1/\gamma$. Be-

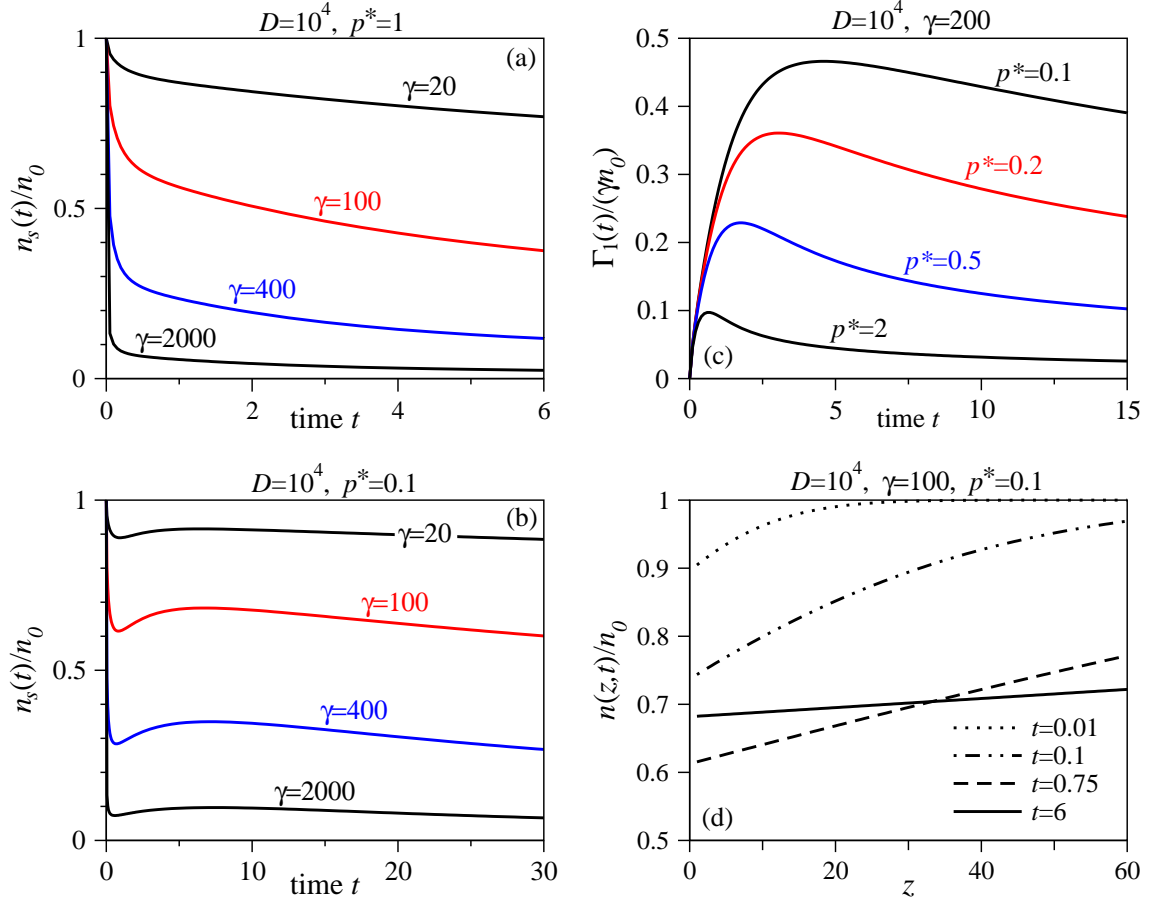


FIG. 4: Densities for $N = 1$. (a) The sublayer density n_s as a function of time, for various values of the dimensionless adsorption rate γ . The other parameters are fixed at $D = 10^4$ and $p^* = 1$. (b) The sublayer density n_s for $D = 10^4$, and $p^* = 0.1$. Note the bump in concentration imparted by the slow annihilation rate p^* . (c) The surface concentration $\Gamma_1(t)$ for various p^* with $D = 10^4$ and $\gamma = 200$. (d) The bulk density profiles $n(z, t)$ as a function of position z at times $t = 0.01, 0.1, 0.75$, and 6 .

yond this transient, the outer solution corresponding to setting $dn_s/dt = 0$ on the left hand side of Eq. 9 holds. Complete particle depletion near the surface occurs in dimensions less than two because there is no bounded steady-state solution to the diffusion equation and the depletion zone moves away from the interface for all times as shown in Fig. 4(d). Despite free diffusion, the bulk is unable to sustain a particle source near the surface as is known from classic diffusion theory [25]. The replenishment at small annihilation rates p^* also manifests itself in the bulk. In the case shown in Fig. 4(d), as time increases from $t = 0.75$ to $t = 6$, the bulk concentration near the interface recovers before ultimately decreasing according to Eq. 19.

For general N , the eigenvectors and eigenvalues must be explicitly computed. However, if we assume that the forward surface reactions rates $p_i = p^* = p$ are all equal, and that all backward rates $q_i = 1$

are also equal, the eigenvalues and eigenvectors can be found explicitly [26, 27] as $\lambda_m = -(p + 1) + 2\sqrt{p} \cos\left(\frac{m\pi}{N+1}\right)$ and $(v_j^m)^2 = \frac{2}{N+1} \sin^2\left(\frac{j m \pi}{N+1}\right)$.

In Figures 5(a-b), we plot n_s as a function of N for uniform $q = 1$ and uniform p . For small p , the surface kinetics is a highly biased random walk away from Γ_N toward Γ_1 , resulting in a larger n_s . Both small p and large N , hinder the annihilation process and impart a more reflective character to the interface. After initial transients, both n_s and the surface concentrations Γ_i maintain a high level for a long time before dissipating. Larger N also effectively trap surface material in the surface reservoir Γ_i . The relative amounts of Γ_i for $N = 4$ are shown in Fig. 5(b). For the small $p = 0.1$ used, most of the surface density lies in the initial species Γ_1 , decreasing in the latter species.

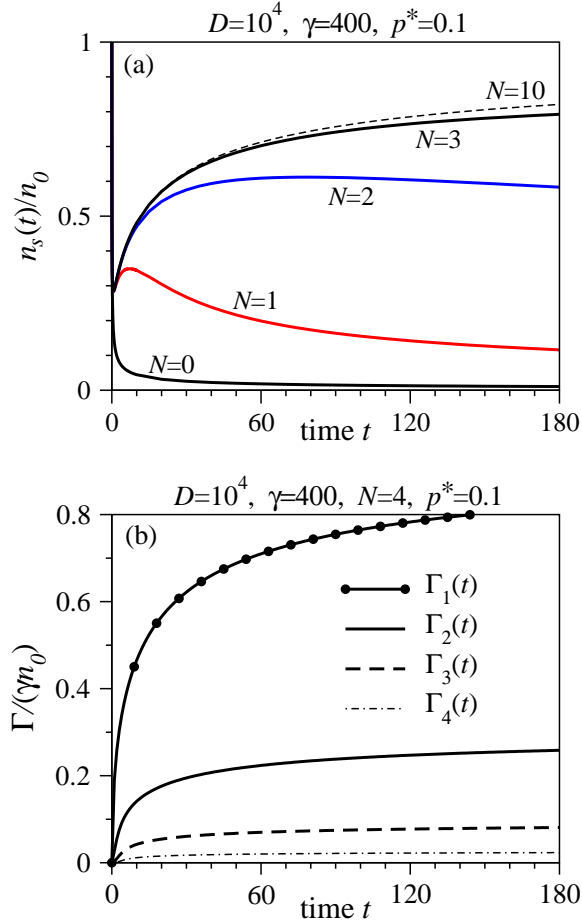


FIG. 5: Dependence of surface quantities on number of steps N in the surface reaction scheme. (a) The sublayer density n_s as N is increased. The initial rapid fall from $n_s/n_0 = 1$ is imperceptible on this scale. (b) The surface concentrations Γ_i as a function of time for $N = 4$.

III. SUMMARY AND CONCLUSIONS

We derive an effective, integro-differential equation for the boundary condition of a simple diffusion process. The effects of intermediate chemical steps at the boundary are described by a delay kernel that can be decomposed using Laplace transforms. This kernel is an explicit function of the eigenvalues and eigenvectors of the surface reaction transition matrix. Our results suggest that measurement of a few quantities, such as fluorescence monitoring of the sublayer density [28], can be used to reconstruct the principal components of $K(t)$. This approach can be used to probe qualitative features of the surface kinetics important in modeling cell membrane signaling and viral infection, where a sequence of chemical steps at the surface are required before initiation of signaling or viral fusion. In HIV infection,

the initial adsorption rate would be proportional to the surface CD4 concentration, and the subsequent rates in the reaction scheme in Fig. 2 would depend on the coreceptor concentrations, their surface mobilities, as well as the effects of cooperative binding [15]. All of these physical attributes are encoded in the distribution of eigenvalues and eigenvectors of \mathbf{M} .

For simple linear reaction schemes on a flat surface, we find explicit dependences of the surface concentrations Γ_i and sublayer concentrations on the eigenvalues and eigenvectors of the transition matrix. For smaller annihilation rates p^* , and at least one ($N \geq 1$) surface intermediate, we find that the surface concentration persists and can replenish the bulk concentrations n_s after its initial decay. The depletion zone in the bulk can also recover. Delays that induce instabilities in dynamical systems have been well established [29]. Here, although the delay occurs in a boundary condition, we observe nonmonotonic behavior arising in the bulk concentrations as well. This rebounding effect is also apparent if one differentiates Eq. 9 with respect to time, giving a second order, harmonic oscillator-like equation, plus a dissipative coupling to the bulk concentration.

Whether the surface concentration or the bulk concentration near the surface vanishes at long times depends on the surface kinetics as well as geometry. If the combined surface kinetics towards annihilation is slow relative to bulk diffusion, the decay of the sublayer concentration n_s can be extremely slow. Similarly, if the number of surface states is large, there is an effective delay to annihilation and a higher probability that a surface species can detach and replenish the sublayer concentration. This effect is very sensitive to the annihilation rate p^* and the size of the reaction N and can keep the subsurface concentration high for essentially all times.

The approach presented differs from the treatments of Ward and Tordai and others since we first use a linear model for the time rate of change of the initially adsorbed species Γ_1 , rather than eliminating the bulk diffusion equation. In applications such as surfactant adsorption, the surface concentration Γ can be appreciable and suppress additional adsorption. If surface species Γ_i has molecular area a_i , an adsorption term including steric exclusion would be $\gamma n_s(1 - \sum_{i=1}^N a_i \Gamma_i)$. The surface rate equations remain linear in Γ , but with a time-dependent transition matrix \mathbf{M} . The effective boundary condition Eq. 9 is now nonlinear in $n_s(t)$ through $F[n_s]$. However, for many biochemical applications (such as cell signalling and virus adsorption and entry) the total surface concentration is low such that $\sum_{i=1}^N a_i \Gamma_i \ll 1$ and the adsorption term can be linearized. In our one-dimensional analysis,

as long as N is not too large and there is an appreciable annihilation process, the surface concentrations all vanish in time. The dependence of finite surface concentrations on the surface kinetics in higher dimensions can also be treated with similar analysis. For example, in three dimensions, the sublayer concentration approaches a positive value $n_s(t \rightarrow \infty) = n_0(1 - \frac{\gamma K_0}{D + \gamma K_0})$. Finally, we expect positive eigenvalues $\lambda_m > 0$ of \mathbf{M} to have a striking effect on the transport. A surface source of parti-

cles may describe virus replication within the living cell substrate (see Fig. 1) and be a simple model for re-release of virus back into the bulk phase.

The authors thank Benhur Lee for stimulating discussions. TC acknowledges support from the NSF (DMS-0349195), and the NIH (K25AI41935). Part of this work was done during the Cells and Materials Workshop at IPAM/UCLA.

-
- [1] Ward, A. F. H., and L. Tordai. 1946. Time-dependence of Boundary Tensions of Solutions. I. The Role of Diffusion in Time-Effects. *J. Chem. Phys.* 14:453-461.
- [2] Diamant, H., G. Ariel, and D. Andelman. 2001. Kinetics of surfactant adsorption: the free energy approach. *Colloids and Surfaces A*. 183-185:259-276.
- [3] Mulqueen, M., Stebe, K. J., and D. Blankschtein. 2001. Dynamic Interfacial Adsorption in Aqueous Surfactant Mixtures: Theoretical Study. *Langmuir*. 17:5196-5207.
- [4] Lin, S.-Y., McKeigue, K., and C. Maldarelli. 1990. Diffusion-controlled surfactant adsorption studied by pendant drop digitization. *AIChE Journal*. 36:1785 - 1795.
- [5] Berg, H. C. and E. M. Purcell. 1977. Physics of Chemoreception. *Biophys. J.* 20:193-219.
- [6] Beverung, C. W., Radke, C. J., and H. W. Blanch. 1999. Protein adsorption at the oil/water interface: characterization of adsorption kinetics by dynamic interfacial tension measurements. *Biophysical Chemistry*. 81:59-80.
- [7] Ybert, C., and J. M. di Meglio. 1998. Study of Protein Adsorption by Dynamic Surface Tension Measurements: Diffusive Regime. *Langmuir*. 14:471-475.
- [8] Schurr, J. M. 1970. The Role of Diffusion in Bimolecular Solution Kinetics. *Biophys J.* 10:700-716. [PubMed]
- [9] Schurr, J. M. 1970. The Role of Diffusion in Enzyme Kinetics. *Biophys J.* 10:717-727.
- [10] P. Bongrand. 1999. Ligand-receptor interactions. *Rep. Prog. Phys.* 62:921-968.
- [11] Pogorzelski, S. J., Kogut, A. D. 2001. Kinetics of marine surfactant adsorption at an air/water interface. Baltic sea studies. *Oceanol.* 43:389-404.
- [12] Leikina E., Markovic I., Chernomordik L. V. and Kozlov M. M. 2000. Delay of Influenza Hemagglutinin refolding into a Fusion Competent Conformation by Receptor Binding: A Hypothesis. *Biophys. J.* 79:1415-1427.
- [13] Clague, M. J., Schoch, C., and R. Blumenthal. 1991. Delay Time for Influenza Virus Hemagglutinin-Induced Membrane Fusion Depends on Hemagglutinin Surface Density. *J. Virology*. 65:2402-2407.
- [14] *Viral Fusion Mechanics* edited by J. Bentz (CRC Press, Boca Raton FL, 1993)
- [15] Kuhmann, S. E., Platt, E. J., Kozak, S. L., and D. Kabat. 2000. Cooperation of Multiple CCR5 Coreceptors is Required for Infections by Human Immunodeficiency Virus Type I. *J. Virology*. 74:7005-7015.
- [16] Platt, E. J., Durnin, J. P., and D. Kabat. 2005. Kinetic Factors Control Efficiencies of Cell Entry, Efficacies of Entry Inhibitors, and Mechanisms of Adaptation of Human Immunodeficiency Virus. *J. Virology*. 79:4347-4356.
- [17] Myszka, D. G., Sweet, R. W., Hensley, P., Brigham-Burke, M., Kwong, P. D., Hendrickson, W. A., Wyatt, R., Sodroski, J., and M. L. Doyle. 2000. Energetics of the HIV gp120-CD4 binding reaction. *PNAS*. 97:9026-9031.
- [18] Wu, H., Myszka, D. G., Tendian, S. W., Brouillette, C. G., Sweet, R. W., Chaiken, I. M., and W. A. Hendrickson. 1996. Kinetic and structural analysis of mutant CD4 receptors that are defective in HIV gp120 binding. *PNAS*. 93:15030-15035.
- [19] Kwon, Y. J., Hung, G., Anderson, W. F., Peng, C. A., and H. Yu. 2003. Determination of Infectious Retrovirus Concentration from Colony-Forming Assay with Quantitative Analysis. *J. Virology*. 77:5712-5720.
- [20] Jung, L. S., and C. T. Campbell. 2000. Sticking Probabilities in Adsorption from Liquid Solutions: Alkylthiols on Gold. *Phys. Rev. Lett.* 84:5164-5167.
- [21] P. Kisliuk. 1958. The Sticking Probabilities of Gases Chemisorbed on the Surfaces of Solids - II. *J. Phys. Chem. Solids*. 5:78-84.
- [22] Maeda, K., Kato, Y., and Y. Sugiyama. 2002. pH-dependent receptor/ligand dissociation as a determining factor for intracellular sorting of ligands for epidermal growth factor receptors in rat hepatocytes. *J. Controlled Release*. 82:71-82.
- [23] Fritz, J., Katopodis, A. G., Kolbinger, F., and D. Anselmetti. 1998. Force-mediated kinetics of single P-selectin/ligand complexes observed by atomic force microscopy. *PNAS*. 95:12283-12288.
- [24] Alon, R., Hammer, D. A., and T. A. Springer. 1995. Lifetime of the P-selectin-carbohydrate bond and its response to tensile force in hydrodynamic flow. *Nature*. 376:539-542.
- [25] J. Crank. 1975. *The Mathematics of Diffusion*. Oxford University Press.
- [26] Huang, Y., and W. F. McColl. 1997. Analytical Inversion of general tridiagonal matrices. *J. Phys. A*. 30:7919-7933.

- [27] Hu, G. Y. and R. F. O'Connell. 1996. Analytical inversion of symmetric tridiagonal matrices. *J. Phys. A.* 29:1511-1513.
- [28] Lieto, A. M., Cush, R. C. and N. L. Thompson. 2003. Ligand-Receptor Kinetics Measured by Total Internal Reflection with Fluorescence Correlation Spectroscopy. *Biophys. J.* 85:3294-3302.
- [29] N. MacDonald. Biological delay systems: linear stability theory. (Cambridge University Press, Cambridge, 1989).